A Survey of Phased Arrays for Medical Applications

(*Invited Paper*)

Cynthia Furse
Electrical and Computer Engineering, University of Utah, 50 S Campus Drive 3280 MEB
Salt Lake City, Utah 84112
cfurse@ece.utah.edu, www.ece.utah.edu/~cfurse
Phone: (801) 585-7234
Fax: (801) 581-5281

***Abstract*—** This paper presents a survey of phased arrays for a wide variety of medical applications. Medical imaging modalities including tomography, confocal imaging, thermography, and MRI are covered, as well as hyperthermia for treatment of cancer. Arrays include planar, cylindrical, and conformal configurations of many types of antennas including monopoles, dipoles, microstrips, horns, bowties, loops, etc.

***Keywords*—** Antenna Arrays, Medical Imaging, Breast Cancer, Hyperthermia, Magnetic Resonance Imaging (MRI)

I. INTRODUCTION

Antenna arrays have been used for a wide variety of medical applications, most notably imaging and hyperthermia treatment of cancer. These arrays may be phased electronically; however more often the received signals are phased after detection. The arrays can be built of multiple antennas or can be produced synthetically by scanning a single antenna or pair of antennas over the object of interest. Medical applications for phased arrays have borrowed heavily on radar applications such as ground penetrating radar, ultrawideband radar, and synthetic aperture radar. This paper surveys the medical imaging and hyperthermia applications of phased array antennas. Microwave tomography, confocal imaging, thermography, and magnetic resonance imaging are covered in section II. Hyperthermia is covered in section III. Some numerical methods for simulating antenna arrays are surveyed in section IV.

II. ANTENNA ARRAYS FOR MEDICAL IMAGING

One of the most promising uses of antenna arrays in medical applications is for imaging the location of leukemia 0, breast tumours [1] - [25], and cardiac anomalies [26] - [27]. Microwave imaging methods rely on the fact that the electrical properties of normal and malignant tissue are significantly different [28] - [35] and that there is significant variation from tissue to tissue. Location of breast cancer shows particular promise, because the relatively low loss of fatty tissue allows electromagnetic fields to propagate to the tumor and back, and the proximity of the tumor to the outer surface of the body means that the signal does not have more than a few inches to propagate. Two major microwave imaging methods utilize antenna arrays. Tomography [2] - [9] attempts to map a complete electrical profile of the breast, and confocal imaging [10] - [25] maps only the location of significant scatterers. Both of these methods have used antenna arrays made up of wideband elements to send and receive the test signals. Microwave thermography picks up the passive electromagnetic fields from the body [36] - [52]. Magnetic Resonance Imaging (MRI) uses a strong magnetic field to cause the magnetic dipoles in the body to align and precess, gradient fields to control and tip the dipoles and then uses an array of receiving loops to pick up the fields when they relax back to their normal state [59] -[74].

A. Tomography for Breast Cancer Detection

Microwave tomography is used to provide a complete spatial mapping of the electrical properties in the region of interest. During the acquisition phase, an array of antennas surrounds the region of interest. One of the antennas in the array is used to transmit a signal, normally a sine wave [2], set of sine waves [3] -[4], or a broadband signal [5], and all of the other antennas are used to receive the reflected signal. The array is scanned so that each antenna transmits each frequency, and those signals are received by each of the other antennas. After all of the data has been acquired, it is processed by comparing the received data with what would be expected from a simulated model of the region. A numerical "forward model" is used to predict how much power is transmitted from the transmit antenna, passes into and reflects from the breast/tumor model, and is received by the receive antenna. Originally the simulated model is just a good guess for

what might be present, generally a generic breast model with no tumor. The differences between the measured and expected received data are used to modify the original guess to obtain an ideal model that best matches the measured data. This "inversion" is used to predict what model would have produced the measured data.

Microwave tomography for breast cancer has been demonstrated by several groups [2] - [9]. In the Dartmouth system, [2] for instance, sine waves from 300-1000 MHz (being expanded to 3 GHz) are transmitted from a circular array of 16 transmit/receive monopole antennas to produce 2D reconstructed images of the breast. Quarter wave monopole antennas (in the fluid) were built by extending the inner conductor of semi-rigid coax used for this application. Monopoles were chosen, because they are easy to model as a line source in a 2D reconstruction algorithm with high accuracy [2]. Water-filled waveguide apertures have also been used for tomography, however the monopole antennas were found to be as accurate, and easier to build [6]. The accuracy of the tomography approach depends on being able to accurately predict the expected received fields from a given transmit antenna / breast model. The antennas and their locations must be accurately modeled in both the transmit and receive case, as any inaccuracy in the antenna models affect the forward model not once, but twice and has a significant impact on the accuracy of the final solution. Monopole antennas can be very accurately modeled and are a good choice for this application. In addition, monopoles have been found to be excellent radiators when resistively loaded by lossy material, having a return loss of about -10 dB from 100 to 1100 MHz when immersed in saline [6]. Thus, for applications such as medical imaging where it is imbedded in a lossy conducting fluid surrounding the object of interest, simple monopoles demonstrate good radiation properties [2]. One of the key factors in obtaining accurate models of the antenna array is to model each of the inactive array elements as a microwave sink, so that the signal is not re-radiated [7] -[8]. This was accomplished in the numerical model by imposing an impedance boundary condition on a finite diameter around each inactive element. The forward model uses a hybrid boundary element (BEM) and finite element method (FEM). In the hardware, a matched switch was the last element in the switching matrix, so that when the antenna is not radiating, any coupled signal is terminated at the switch. The 32 channel data acquisition system allows each antenna (16 transmit and 16 receive) to act as only a transmitter or receiver, which provides a dynamic range of 130 dB and channel-to-channel isolation of greater than 120 dB.

Since the goal is to identify tumours that have significant dielectric discontinuity from the surrounding tissue, best results will be obtained if they are the primary scatterers in the environment. Blood vessels are also significant scatterers, but these cannot be controlled. They will also show up on a tomographic image. The other major scattering source is the air-skin interface, and this can be controlled. This reflection can be minimized by immersing the antennas and breast in a fluid medium that is electrically similar to breast/skin. Originally saline was used, which is a better match than air, inexpensive and safe, however its relative permittivity is significantly higher than that of fatty breast tissue, and a better matched fluid material is recommended. The monopole antennas are designed to be used in the liquid medium, rather than air, with the conductive fluid providing the resistive loading of the monopoles. The feed system also needs to be designed so that it can be used in fluid. The sealing of the antenna feed system along with the ability to raise and lower the array in parallel with the fluid level was a significant challenge in the system prepared for clinical trials in [6] .

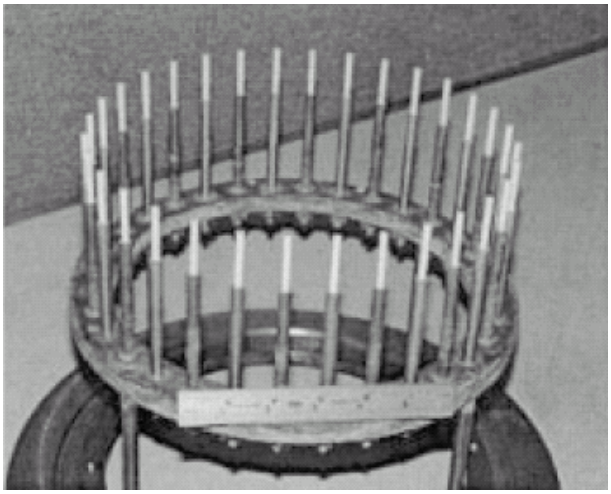

Fig. 1. 2D Monopole array used for tomographic imaging of the breast (from [2] © 2000 IEEE).

For a microwave tomography breast exam, the woman lies with the breast pendant through a hole in the examination table and immersed in the tank of matching fluid. The circuit antenna array of monopoles is also immersed in this fluid and radially surrounds the breast. For each 2D breast scan, signals are transmitted from each antenna and individually received in parallel at the remaining antennas. This is repeated for 12 frequencies over the 300-1000 MHz band. This is repeated for seven vertical array positions on the order of 1cm. The total acquisition time for the 3D image of both breasts is about 15 min. A complete set of seven images at a single frequency can be reconstructed in less than 5 min using a Compaq AlphaServer ES40 68/833.

Microwave tomography has been validated experimentally [9]. The presence of 1.1 or 2.5 cm saline tubes (representing tumours) in excised breast tissue are seen to be clearly visible [8]. Objects as small as 4 mm in diameter have been imaged at 900 MHz [9].

B. Confocal Imaging for Breast Cancer Detection

Confocal imaging for breast cancer detection is another exciting application of antenna arrays in medical imaging. Confocal imaging is similar to ground penetrating radar. Unlike microwave tomographic imaging, this method does not provide a complete electrical mapping of the region of interest. Instead it identifies locations of significant scattering. This method typically uses a single antenna scanned in a flat array pattern above the breast or in a cylindrical pattern around the breast [10]. For planar imaging, the patient lies face up, and the antenna is physically scanned in a plane above the breast [11] - [13]. For cylindrical imaging, the patient lies face down, with the breast extending into a cylindrical tank containing the antenna through a hole in the table [14] - [15]. Matching fluid surrounding the breast, similar to that used for microwave tomography, is suggested in this case. Both methods provide similar results [15]. The confocal imaging process is shown in Fig. 2. One antenna in the array transmits an ultrawideband pulse, which propagates into the breast, where it is reflected off significant electrical discontinuities, and is received in parallel by the other antennas in the array. Knowing the physical spacing between the array elements, the different delays between the transmit antenna, scattering point, and receiving antenna can be calculated geometrically. The received pulses representing a specific point in space can then be time delayed appropriately for each antenna, added up and integrated to indicate the magnitude of the scattered energy from that point in space. This is effectively correlating the signals received from that point at all antennas.

The antennas used for confocal imaging must be ultrawideband and small enough to fit within the relatively small array area. Resolution of less than 1 cm requires a bandwidth of at least 5 GHz. The lossy nature of tissue attenuates high frequency signals, limiting the upper frequency to about 10 GHz. Initially, resistively loaded bowtie were suggested for the planar configuration, [11]-[13], [17], [19], while dipole antennas were suggested for the cylindrical system [14]-[15]. Resistively loaded Vee dipoles have also been proposed [18]. In the cylindrical configuration, and the planar system, a single antenna is scanned over the surface, creating a synthetic antenna aperture. In order to overcome the inherent inefficiency of resistively loaded antennas, a modified ridged horn antenna operating from 1 to 11 GHz has been introduced [20]. Most of the antennas are designed to observe co-polarized reflections from the breast, however using two resistively loaded bowtie antennas in the shape of a Maltese cross has also been proposed to pick up the cross polarized reflections[12]. Cross-polarized reflections from simple tumor models were also examined in [16].

The antenna shown in Fig. 3 [16] consists of two cross polarized bowtie antenna elements, an octagonal cavity behind the bowtie elements, and a metal flange attached to the cavity. The broadband bowties have flare angles of 45°. They are 1.67 cm long, which is a half-wavelength at 3 GHz in fat (similar to breast). The octagonal cavity blocks waves radiated away from the breast.

The cavity is approximated as a circular waveguide filled with fat material for matching and size reduction. The first cutoff frequency is set to be 2 GHz for 2-4 GHz operation. The cavity length is a quarter-wavelength, which is 11 mm at 3 GHz. The flange consists of an inner and outer component, and is designed to block unwanted waves such as surface waves. The antenna performance does not change significantly when the flange size is varied between 10–6.25 cm, therefore, the width of the outer flange is set to be 6.25 cm. The inner flange is designed to prevent possible electric field overshoot at the inner corners of the opening of the octagonal cavity or at the ends of the bowtie elements.

A slotline bowtie antenna shown in Fig. 4 has also been proposed in [22]. The slotline was produced on a high dielectric substrate (Rogers RT-Duroid 6010.2LM, Rogers Corporation, Rogers, CT, USA). The substrate has an ε_r of 10.2 at 10 GHz with a low-loss factor tan δ of 0.0023 and a thickness of 635 μm. The ultra-wideband balun uses a via as a short. The holes for the vias in the balun are drilled and electroplated. The balun and the profile of the antenna are then milled. The bowtie plates are designed to be cut from a 508 μm-thick sheet of copper. To obtain the correct contour of the plates accurately without damaging the fragile antenna board, a steel jig was made by tracing the contour of the antenna board. The bowtie plates were bent along this jig, and then carefully soldered on to the antenna board at right angles. The antenna plates were encased in a dielectric epoxy (Eccostock Hi K Cement, Emerson & Cuming Microwave Products, Randolph, MA, USA) with ε_r =10 for structural support and improved matching.

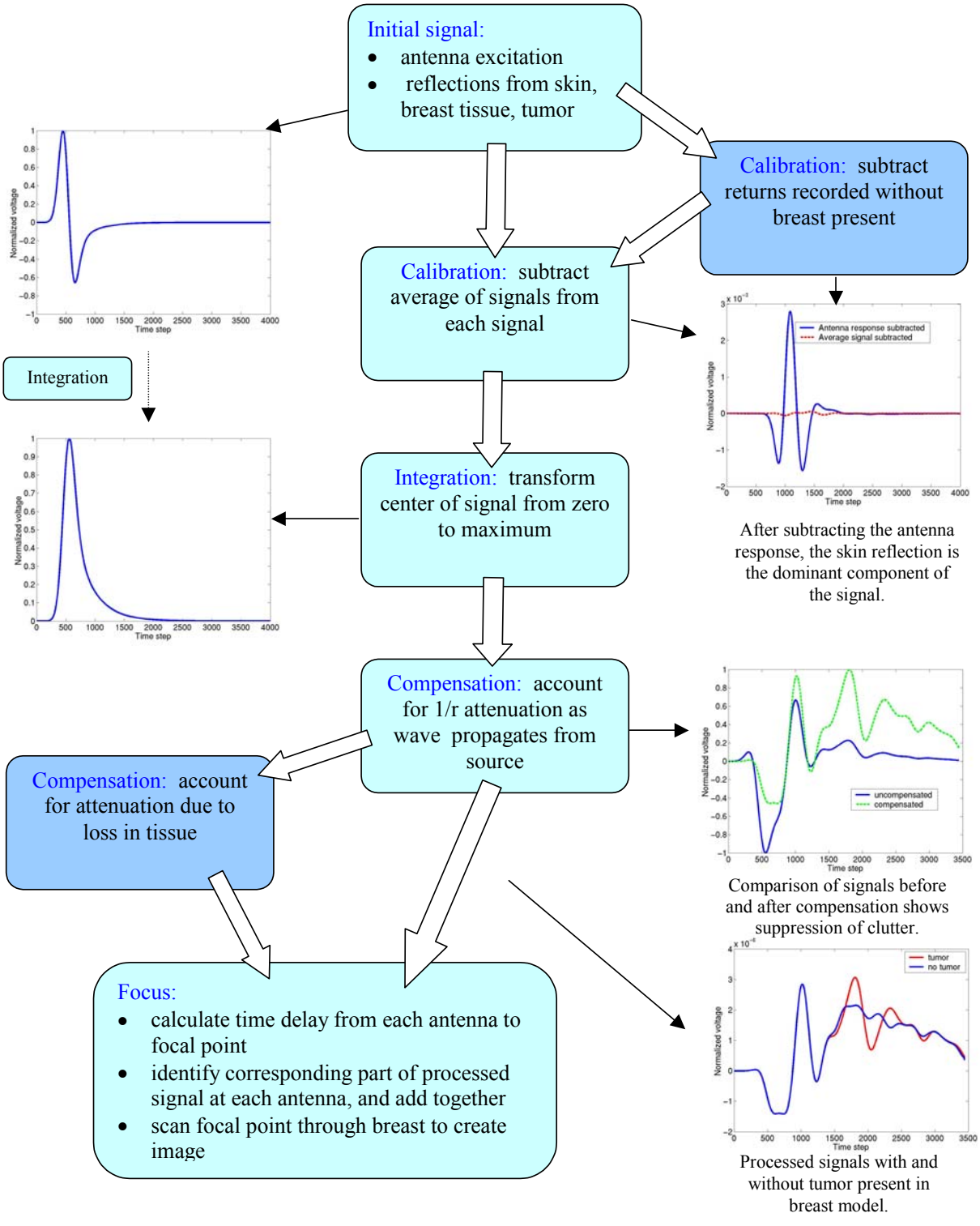

Fig. 2. Confocal Microwave Imaging Process. (From [10] © 2002 IEEE)

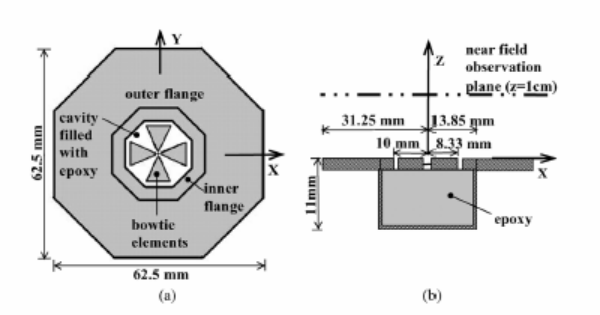

Fig. 3. Cross polarized antenna for confocal imaging. The properties of the substance inside the cavity and the medium outside the antenna are similar to fat (ε_r = 9; σ = 0:2 S/m). (From [16] © 2005 IEEE)

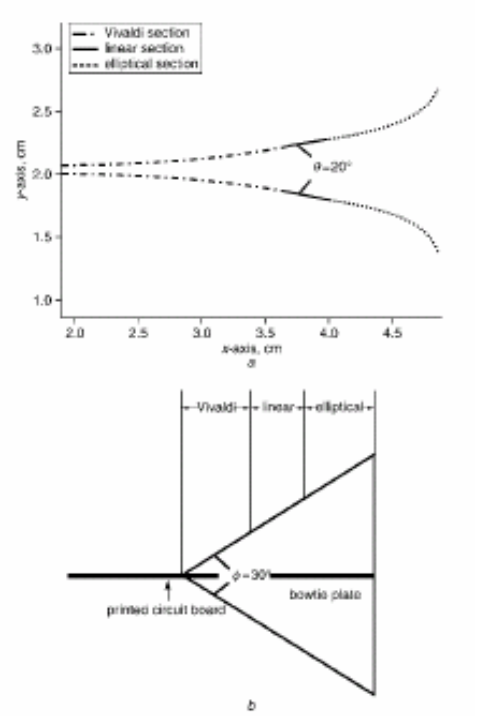

Fig. 4. Slotline Antenna and a Top view with Vivaldi, linear and elliptical sections indicated b Side view with Vivaldi, linear and elliptical sections and bowtie plates. (From [22] © 2005 IEEE)

A resistively loaded monopole antenna shown in Fig. 5 suitable for use in the cylindrical system was proposed in [25]. Based on the Wu–King design [75] - [76] this antenna was designed to be useable from 1to10 GHz immersed in canola oil (ε_r = 3.0) for matching to breast tissue. The antenna is fabricated using high-frequency chip resistors (Vishay 0603HF) (Malvern, PA) soldered to a high-frequency substrate (Rogers RO3203 series) (Rogers Corporation, Chandler, AZ). The substrate (ε_r = 3.02 and σ= 0.001 S/m) has electrical properties similar to those of the canola oil. The antenna is soldered to a subminiature A (SMA) connector and attached to a metal plug for connection into the oil-filled test canister.

The cylindrical confocal imaging system has been experimentally tested [77], [23], [25]. Simulated tumours of diameter 1 cm have been detected using a system that represents the skin as 2D and the tumor model as 3D.

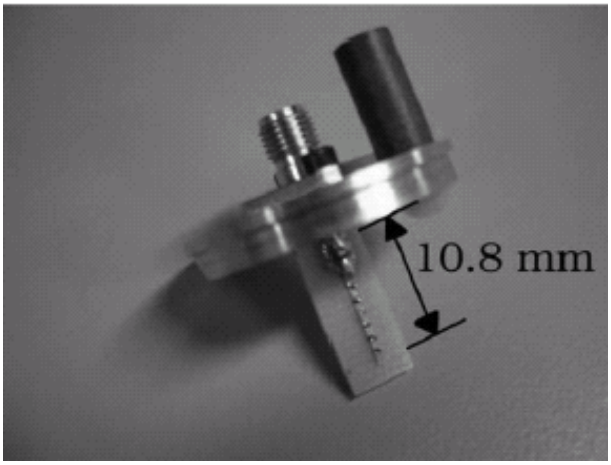

Fig. 5. Fabricated resistively loaded monopole antenna soldered to an SMA connector and attached to a metal plug. (From [25] © 2005 IEEE)

C. Microwave Radiometry

Microwave radiometry is a passive method where the natural electromagnetic radiation or emission from the body is measured to allow detection or diagnosis of pathogenic conditions in which there are disease-related potentials [36] -[37]. This method has been proposed for detection of breast cancer [40], [50], [51] and brain cancer [41], in which the metabolism of cancer cells increases the localized temperature 1-3°C. This method has also been used for fluid and blood warming [37], detection or rheumatology [39], and for monitoring of temperature rise during hyperthermia treatment [38].

Typical antennas include open ended rectangular waveguides [42]-[45], small-loop antennas [47], or a horn antenna with a dielectric lens [48]. Working around 3 GHz, all of these antennas have radiation patterns that have minimal penetration into the body, thus strongly weighting them to monitoring of surface temperatures. [49], [52] Increased focus and therefore better spatial accuracy was obtained with an array of six rectangular aperture antennas filled with low loss dielectric (ε_r = 25), which were scanned over the object of interest in an overlapping pattern. Preliminary results indicated promise for location of breast tumours [50] - [51].

D. Magnetic Resonance Imaging

Magnetic Resonance Imaging (MRI) uses a very strong magnetic field (0.5T, 1.5T, 3T, 4T, 7T, perhaps in the future 8T) to make the magnetic dipoles in the body precess (line up). When they are released, a set of receiver coils picks up the magnetic field created when these dipoles return to their normal orientations (position may change a lot as in blood imaging, diffusion etc.). The relaxation properties of the different tissues effects the relative received signal intensities and a 3D map of the body can be produce. There are two basic types of receiver coils used for MRI. Volume coils, such as the quadrature birdcage head coil shown in Fig. 6 [53] and whole body coils [54] are used for imaging large sand deep anatomic structures volume of the body and provide homogeneous field profiles.. For high resolution applications that are more localized, such as angiographic imaging, hypocampus imaging, and functional imaging, in which the object features are very small, volume coils pick up less signal and more noise, thus having a lower signal to noise ratio and poor quality images. Modifications of the birdcage, such as the use of an RF reflector or "endcap" [53], and modified shapes such as the elliptical [55], or "dome" [56], [57] coils, have been developed. Smaller volume surface coils [58] have been shown to improve image quality, particularly when combined into phased arrays [59]-[67] such as the one shown in Fig. 7. Phased array coils are closer to the area of interest so pick up larger signal strength and are smaller so pick up less noise, thus having higher signal to noise ratio (SNR). Adjacent elements are overlapped so that the mutual inductance between coils is zero. The coupling between non-adjacent elements is greatly decreased using, very low input impedance preamplifiers. Coil to coil interactions are minimized for optimal SNR [59]. Part of the price for this improved image quality is the complexity of the receiver and data acquisition system, as each antenna element requires a separate receiver channel. The image processing is also more computationally expensive, as the signal from each antenna is weighted depending on its proximity to the target region (and hence expected relative SNR), phase shifted, and combined with the other similarly processed signals. Among the practical considerations that are challenging with phased array coils are the expense of additional receiver channels (or the limited number of channels on existing scanners), data acquisition time and the limited field of view, particularly for applications where the region of interest (an arterial occlusion, for instance) may not be precisely known and is therefore easy to miss. Phased-array coils have been used for numerous magnetic resonance angiography (MRA) applications including peripheral [68], [69] abdominal, intracranial and carotid imaging [70] - [72]. Recent coil designs have started to integrate phased-array elements into volume-like coils with the ability to control how the image is constructed to achieve maximum image quality [73], [74]. For these applications, the coil array functions much like the phased array in a synthetic aperture radar application. The image quality for the different coil types and configurations depends strongly on the application. The optimal image construction algorithm depends strongly on the application and region of interest, making the flexibility of being able to synthetically develop large or small subarrays very attractive.

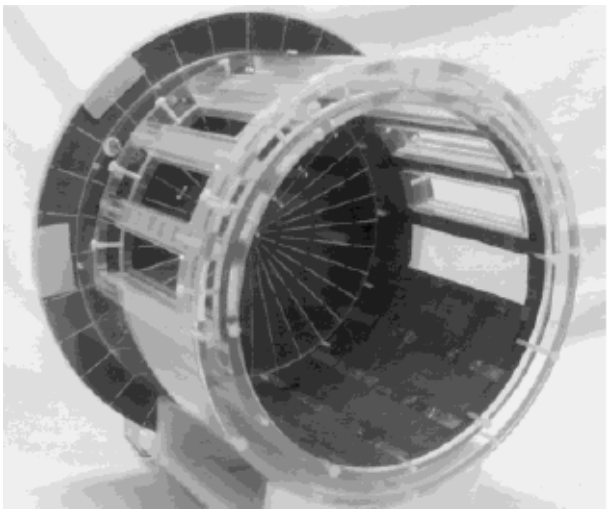

Fig. 6. Quadrature birdcage coil with endcap used for whole-volume head imaging. (Reprinted with permission from [53])

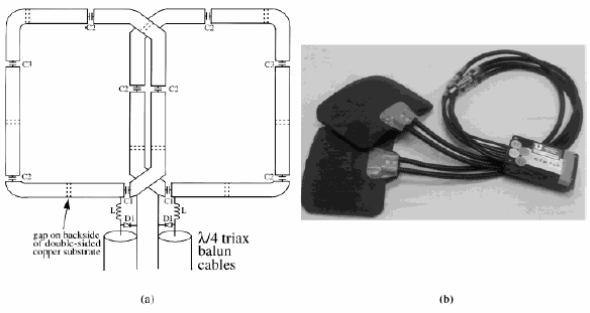

Fig. 7. (a) Two element phased-array coil design. Dashed lines indicate the breaks in the underside of the double-sided copper section of the coil. (b) Image of finished phased array coils (enclosed in foam) with triax balun cables and phased-array port connector box. (Reprinted with permission from [53])

III. ANTENNA ARRAYS FOR HYPERTHERMIA CANCER TREATMENT

Hyperthermia (HT) [78], [79] is a method of treating cancer by heating the body. The tissue is typically heated to 41-45°C for 30-60 min. Often, this involves focusing the energy on the tumor region, relying on the tumor to be more sensitive to heat than the surrounding healthy tissues. HT has also been shown to increase the effectiveness of radiation or chemotherapy [80] - [81]. The most commonly used frequencies for hyperthermia are 433, 915, and 2450 MHz. The type of antenna or antenna array used for HT depends on if it is to be administered superficially, interstitially, or deep-body.

Superficial HT applicators include microstrip [82], waveguide [83], current sheets [84], and the dual concentric conductor antenna, or DCC shown in Fig. 8 [85] -[87]. The DCC is particularly attractive, because it can be easily fabricated on flexible printed circuit board material, which makes it easy to conform to virtually any part of the human body. The DCC aperture is a ring-slot configuration fed simultaneously on all four sides. Prediction and optimization of the heating is normally done by analyzing the near fields of the antenna (the heating region) with numerical methods [86].

Interstitial applicators for HT are typically monopole antennas made from coaxial cables with the center conductor extending beyond the outer ground shield of the cable [88]. These antennas have a tear-drop shaped radiation pattern, so the majority of the heating is near the feedpoint of the antenna (where the ground shield stops), leaving the tip of the antenna extended beyond the useable heating range. The heating distribution can be made more uniform by varying the width of the conductor [89], [90] or adding a choke to the antenna [91]. The heating pattern can be adjusted within the array by phasing the antenna elements [89], [90] or by using nonuniform insulation [92]. Several interstitial applicators were simulated in [93].

Deep body HT applicators are generally based on annular phased arrays (APA) of waveguides [79], coaxial TEM apertures [94], printed antennas [88],[95] and induction systems[96]. Originally, APA systems contained only one ring of 2-D applicators surrounding the patient [97]. The ring could be scanned vertically. Significant improvement with a true 3-D HT system with the applicators vertically offset has been observed [88]. The first clinically used 3-D-type applicator is the SIGMA-Eye applicator (BSD Medical Corp., SLC, UT [98]). A detailed description of this applicator and different numerical antenna feed models can be found in [98],[99].

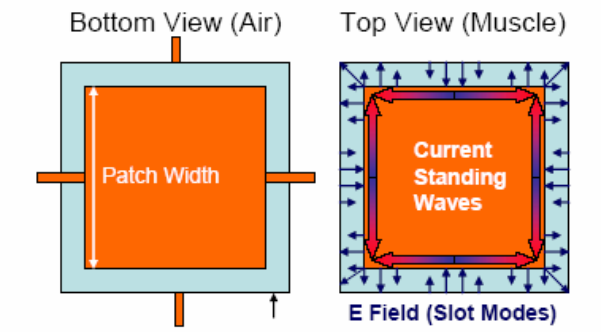

Fig. 8. DCC antenna geometry, E fields in the ring slot and edge currents. (From [85] © 2003 IEEE)

Among the ongoing antenna design challenges in this area is the design of antennas that can be used to also monitor temperature and administer radiation therapy [87], [95], [100]. One prototype combination device is shown in Fig. 9 and another in Fig. 10. Another research area is the use of optimization approaches to predict and control the heating pattern [101], [102]

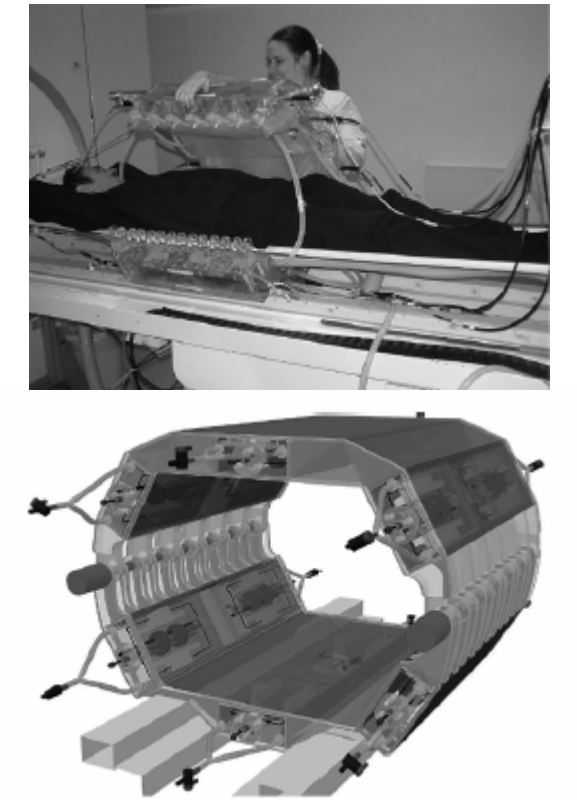

Fig. 9. A prototype of the new Berlin MR-compatible Water-Coated Antenna Applicator (WACOA). (From [100] © 2005 IEEE)

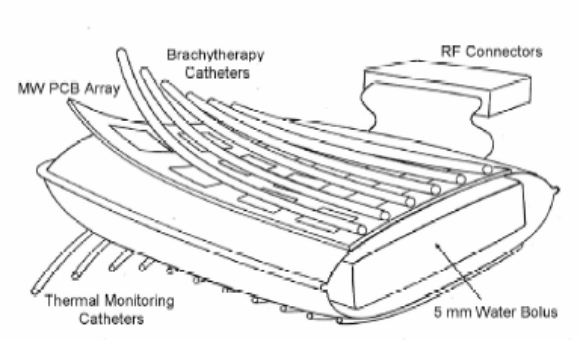

Fig. 10. Schematic of combination applicator showing component parts: parallel catheter arrays for brachytherapy sources and thermal mapping sensors, PCB antenna array, and water coupling bolus. (From [95] © 2004 IEEE)

IV. NUMERICAL SIMULATION METHODS FOR BIOMEDICAL ARRAYS

Several methods for analyzing antenna arrays for medical applications exist. For simple cases where the biological structure can be approximated as uniform or by very simple models such as layers or cylinders, classical methods such as analytical analysis [53], [103] or method of moments [104]-[105] can be used. If the structure of the body varies so much that anatomically-precise modeling is rendered imprecise by variation between individuals, these simple analyses can be used to determine an optimal array design for the range of expected variation between individuals. An example of this was done in [106] for design of coils for vascular MRI. Another example when the body can be modeled as near-uniform is in the case of arrays for hyperthermia of the brain. In [89] stepped-impedance dipoles were modeled using method of moments in an homogenous brain with a localized (non-homogenous) tumor. Method of moments with a simple pulsed basis function (which is the most numerically efficient form) has limitations for heterogeneous models, however, due to artificial charge build up on the dielectric interfaces. [107] Higher order basis functions can overcome this limitation, although the computational complexity is significantly increased [108] - [109]. In addition, the method of moments is very computationally expensive when heterogenous models are evaluated. It requires N logN computations, where N is the number of cells in the model, including those making up the heterogeneous object.

A more efficient method for calculation of heterogeneous objects is the finite difference time domain (FDTD) method, which has lead to its tremendous popularity for numerical bioelectromagnetic calculations. For example, the interstitial array of hyperthermia applicators simulated using method of moments in [89] was simulated with a fraction of the computational resources using FDTD in [90]. Several individual hyperthermia applicators have been simulated using FDTD in [93]. FDTD requires N^2 computations, where N is a cell in the (normally cubical) FDTD grid. Unlike method of moments, every cell in space (including at least a minimal amount of air surrounding the model) must be included in the discrete model, so the total number of cells, N, is likely to be larger. However the significant improvement in computational efficiency generally makes this tradeoff favor FDTD for bioelectromagnetic simulations. Complete detailed analysis of breast cancer imaging modalities was also done with FDTD [2]-[25], as well as hyperthermia systems [97], and evaluation of cell phones (including those with dual antennas) near the human head. [110],[111] Antennas for implantation in the body (mostly microstrip or PIFA types) have been simulated with FDTD and in some cases optimized with genetic algorithms [112]. Deep hyperthermia applicators (annular phased arrays) have been simulated extensively with FDTD [113] -[115].

Several FDTD developments have been important for bioelectromagnetic simulations including the development of frequency-dependent methods $(FD)^2TD$, [116] low frequency FDTD methods, [117] efficient FDTD computation, [118] and evaluation of temperature using the bioheat equation [115].

Model development is one of the significant challenges of numerical bioelectromagnetics. Models have progressed from the prolate spheroidal models of the human used during the 1970s [119] to roughly 1cm models based on anatomical cross sections used during the 1980s [120] to a new class of millimeter-resolution MRI-based models of the body that have been the hallmarks of research since the 1990s [121]-[124]. Today probably the most widely used models are derived from the Visible Man Project [125].

Once a tissue-segmented model has been chosen, the electrical properties of the tissues are defined. The properties of human tissue change significantly with frequency, so it is essential to use data accurately measured at the frequency of interest. There is a wide range of published data on measured tissue properties [28] -[35], [119], [126]-[129], and work is still underway to measure and verify these properties. These and other references are electronically searchable at [130].

Periodic boundary conditions are available for method of moments [131], [132] and the FDTD method [133] - [138] for predicting array behavior from

evaluation of a single antenna in the array. These may have application in antenna arrays for medical applications; however they have not been used in this application space yet. This is no doubt due at least in part to the fact that the nearby human body is neither uniform nor periodic in shape.

VI. CONCLUSIONS

The applications for phased arrays in medicine have borrowed strongly from other applications of phased arrays, particularly those seen in radar. Imaging methods including tomography, confocal imaging, thermography, and MRI provide enhanced medical imaging. Hyperthermia treatments often improve the outcome of radiation and chemotherapy for cancer treatment. A wide variety of antennas have been used in these arrays, and the arrays have been produced either physically or synthetically by scanning a single antenna or pair of antennas over the region of interest. The arrays have been phased either electronically, or (more commonly) by time delaying the received signals during recombination. Design challenges for these applications include making the antennas small enough to be physically useable, coupling the signal to the body with minimal reflection, using low enough frequency to penetrate lossy biological material yet high enough frequency to obtain good resolution. Among the current research challenges are optimized design of the arrays for a variety of configurations and integration of other technologies (radiation therapy and temperature monitoring, for instance) with the antenna design. Applications for phased array antennas promise continued growth in the medical arena.

ACKNOWLEDGEMENTS

The author gratefully acknowledges the assistance of Dr. Rock Hadley for contributions to the MRI section of this paper.

REFERENCES

[1] D. Colton and P. Monk, “A new approach to detecting leukemia: Using computational electromagnetics,” *IEEE Trans. Comput. Sci. Eng.*, vol.2, pp. 46–52, winter 1995.

[2] P. M. Meaney, M. W. Fanning, D. Li, S. P. Poplack, and K. D. Paulsen, “A clinical prototype for active microwave imaging of the breast,” *IEEE Trans. Microwave Theory Tech.*, vol. 48, pp. 1841-1853, Nov. 2000.

[3] W. C. Chew and J. H. Lin, “A frequency-hopping approach for microwave imaging of large inhomogeneous bodies,” *IEEE Microwave Guided Wave Lett.*, vol. 5, pp. 439–441, Dec. 1995.

[4] O. S. Haddadin and E. S. Ebbini, “Imaging strongly scattering media using a multiple frequency distorted Born iterative method,” *IEEE Trans. Ultrason., Ferroelect., Freq. Contr.*, vol. 45, pp. 1485–1496,Nov. 1998.

[5] Q. Fang, P. M. Meaney, and K. D. Paulsen, “Microwave image reconstruction of tissue property dispersion characteristics utilizing multiple-frequency information,” *IEEE Trans. Microwave Theory Tech.*, vol. 52, pp. 1866-1875, Aug. 2004.

[6] P. M. Meaney, K. D. Paulsen, A. Hartov, and R. C. Crane, “An active microwave imaging system for reconstruction of 2-D electrical property distributions,” *IEEE Trans. Biomed. Imag.*, vol. 42, pp. 1017–1026, Oct. 1995.

[7] K. D. Paulsen and P. M. Meaney, “Compensation for nonactive array element effects in a microwave imaging system: Part I—Forward solution vs. measured data comparison,” *IEEE Trans. Med. Imag.*, vol. 18, pp. 496–507, June 1999.

[8] P. M. Meaney, K. D. Paulsen, M. W. Fanning, and A. Hartov, “Nonactive antenna compensation for fixed-array microwave imaging: Part II—Imaging results,” *IEEE Trans. Med. Imag.*, vol. 18, pp. 508-518, Jun. 1999.

[9] P. M. Meaney, K. D. Paulsen, A. Hartov, and R. K. Crane, “Microwave imaging for tissue assessment: Initial evaluation in multitarget tissue-equivalent phantoms,” *IEEE Trans. Biomed. Eng.*, vol. 43, pp. 878-890, Sept. 1996.

[10] E. C. Fear, S. C. Hagness, P. M. Meaney, M. Okieniewski, and M. Stuchly, “Enhancing breast cancer detection using near field imaging,” *IEEE Microwave Magazine,* pp. 48-56, March 2002.

[11] S. C. Hagness, A. Taflove, and J. E. Bridges, “Two-dimensional FDTD analysis of a pulsed microwave confocal system for breast cancer detection: Fixed-focus and antenna-array sensors,” *IEEE Trans. Biomed. Eng.*, vol. 45, pp. 1470–1479, Dec. 1998.

[12] S. C. Hagness, A. Taflove, and J. E. Bridges, “Three-dimensional FDTD analysis of a pulsed microwave confocal system for breast cancer detection: Design of an antenna-array element,” *IEEE Trans. Antennas Propagat.*, vol. 47, pp. 783–791, May 1999.

[13] X. Li and S. C. Hagness, “A confocal microwave imaging algorithm for breast cancer detection,” *IEEE Microwave Wireless Comp. Lett.*, vol. 11, pp. 130–132, Mar. 2001.

[14] E. Fear and M. Stuchly, “Microwave system for breast tumor detection,” *IEEE Microwave Guided Wave Lett.*, vol. 9, pp. 470–472, Nov. 1999.

[15] E. C. Fear and M. A. Stuchly, "Microwave detection of breast cancer," *IEEE Trans. Microwave Theory Tech.*, vol. 48, pp. 1854–1863, Nov. 2000.

[16] X. Yun, E. C. Fear, and R. H. Johnston, "Compact Antenna for Radar-Based Breast Cancer Detection," *IEEE Trans. Antennas and Propagation,* vol. 53, no. 8, pp. 2374 -2380, Aug. 2005.

[17] S. C. Hagness, A. Taflove, and J. E. Bridges, "Wideband ultralow reverberation antenna for biological sensing," *Electronic Lett.*, vol. 33, no. 19, pp. 1594–1595, Sep. 1997.

[18] M. A. Hernandez-Lopez, M. Pantoja, M. Fernandez, S. Garcia, A. Bretones, R. Martin, and R. Gomez, "Design of an ultra-broadband V antenna for microwave detection of breast tumors," *Microw. Opt. Tech. Lett.*, vol. 34, no. 3, pp. 164–166, Aug. 2002.

[19] E. C. Fear and M. A. Stuchly, "Microwave breast tumor detection: Antenna design and characterization," *IEEE Antennas Propag. Symp. Dig.*, vol. 2, pp. 1076–1079, 2000.

[20] X. Li, S. C. Hagness, M. K. Choi, and D. W. W. Choi, "Numerical and experimental investigation of an ultrawideband ridged pyramidal horn antenna with curved launching plane for pulse radiation," *IEEE Antennas Wireless Propag. Lett*., vol. 2, pp. 259–262, 2003.

[21] X. Yun, E. C. Fear, and R. H. Johnston, "Radar-based microwave imaging for breast cancer detection: Tumor sensing with cross-polarized reflections," *IEEE Antennas Propag. Society Symp. Dig*., vol. 3, pp. 2432–2435, 2004.

[22] C. J. Shannon, E. C. Fear, and M. Okoniewski, "Dielectric-filled slotline bowtie antenna for breast cancer detection," *Electronics Letters*, vol. 41, no. 7, March 2005.

[23] J. M. Sill and E. C. Fear, "Tissue sensing adaptive radar for breast cancer detection: A study of immersion liquid," *Electronics Letters*, vol. 41, no. 3, pp. 113–115, Feb. 2005.

[24] J. M. Sill and E. C. Fear, "Tissue sensing adaptive radar for breast cancer detection: Preliminary experimental results," *IEEE MTT-S Int. Microwave Symp. Dig*., Long Beach, CA, June 2005.

[25] J. M. Sill and E. C. Fear, "Tissue Sensing Adaptive Radar for Breast Cancer Detection—Experimental Investigation of Simple Tumor Models," *IEEE Trans. Microwave Theory Tech.*, vol. 53, no. 11, pp. 3312-3319, Nov. 2005.

[26] S. Y. Semenov, A. E. Bulyshev, A. E. Souvorov, R. H. Svenson, Y. E. Sizov, V. Y. Borisov, V. G. Posukh, I. M. Kozlov, A. G. Nazarov, and G. P. Tatsis, "Microwave tomography: Theoretical and experimental investigation of the iteration reconstruction algorithm," *IEEE Trans. Micr. Theory Tech.*, vol. 46, pp. 133–141, Feb. 1998.

[27] S. Y. Semenov, R. H. Svenson, A. E. Bulyshev, A. E. Souvorov, A.G. Nazarov, Y. E. Sizov, V. G. Posukh, and A. Pavlovsky, "Three-dimensional microwave tomography: Initial experimental imaging of animals," *IEEE Trans. Biomed. Eng*., vol. 49, pp. 55–63, Jan. 2002.

[28] C. Gabriel, S. Gabriel, and E. Corthout, "The dielectric properties of biological tissues: I. Literature survey," *Phys. Med. Biol*., vol. 41, pp. 2231-2249, 1996.

[29] S. Gabriel, R. W. Lau, and C. Gabriel, "The dielectric properties of biological tissues: II. Measurements on the frequency range 10 Hz to 20 GHz," *Phys. Med. Biol*., vol. 41, pp. 2251-2269, 1996.

[30] S. Gabriel, R. W. Lau, and C. Gabriel. "The dielectric properties of biological tissues: III. Parametric models for the dielectric spectrum of tissues," *Phys. Med. Biol*., vol. 41, pp. 2271-2293, 1996.

[31] K. R. Foster and H. P. Schwan, "Dielectric properties of tissues and biological materials: A critical review," *Crit. Rev. Biomed. Eng*., vol. 17, pp. 25-104, 1989.

[32] S. S. Chaudhary, R. K. Mishra, A. Swarup, and J. M. Thomas, "Dielectric properties of normal and malignant human breast tissues at radiowave and microwave frequencies," *Indian J. Biochem. Biophys*., vol. 21, pp. 76-79, 1984.

[33] A. J. Surowiec, S. S. Stuchly, J. R. Barr, and A. Swarup, "Dielectric properties of breast carcinoma and the surrounding tissues," *IEEE Trans. Biomed. Eng.*, vol. 35, pp. 257-263, Apr. 1988.

[34] W. T. Joines, Y. Z. Dhenxing, and R. L. Jirtle. "The measured electrical properties of normal and malignant human tissues from 50 to 900 MHz," *Med. Phys*., vol. 21, pp. 547-550, 1994.

[35] A. M. Campbell and D. V. Land, "Dielectric properties of female human breast tissue measured in vitro at 3.2 GHz," *Phys. Med. Biol*., vol. 37, pp. 193-210, 1992.

[36] K. L. Carr, "Microwave radiometry: Its importance to the detection of cancer," *IEEE Trans. Microwave Theory Tech.*, vol. 37, no. 12, pp. 1862-1869, Dec. 1989.

[37] K. L. Carr, "Radiometric sensing," *IEEE Potentials*, pp. 21-25, April/May 1997.

[38] L. Dubois, J. – P. Sozanski, V. Tessier, J. –C. Camart, J. –J. Fabre, J. Pribetich, and M. Chiv, " Temperature Control and Thermal Dosimetry by Microwave Radiometry in Hyperthermia," *IEEE*

Trans. Microwave Theory Tech., vol. 44, no. 10, pp. 1755-1761, Oct. 1996.

[39] S. M. Fraser, D. V. Land, and R. D. Sturrock, "Microwave Thermography - an Index of Inflammatory Disease," *Br. J. Rheumatology*, vol. 26, pp. 37-39, 1987.

[40] B. Bocquet, J. C. Van de Velde, A. Mamouni, and Y. Leroy, "Microwave radiometric imaging at 3 GHz for the exploration of breast tumours," *IEEE Trans. Microwave Theory Tech*., vol. 38, pp. 791-793, 1990.

[41] J. Robert, J. Edrich, P. Thouvenot, M. Gautherie, and J. M. Escanye, "Millimeter wave thermography: Preliminary clinical finding on head and neck diseases," *J. Microwave Power*, vol. 14, 1979.

[42] K. L. Carr, A. M. ElMahdi, and J. Schaeffer, "Dual mode microwave system to enhance early detection of cancer," *IEEE Trans. Microwave Theory Tech*., vol. 29, pp. 256-260, 1980.

[43] E. A. Cheever, J. B. Leonard, and K. R. Foster, "Depth of penetration of fields from rectangular apertures into lossy media," *IEEE Trans. Microwave Theory Tech*., vol. 35, pp. 865-867, 1987.

[44] J. Audet, J. C. Bolomey, C. Pichot, D. D. n'Guyen, M. Robillard, M. Chive, and Y. Leroy, "Electrical characteristics of waveguide applicators for medical applications," *J. Microwave Power*, vol. 15, pp. 177-186, 1980.

[45] A. W. Guy, "Electromagnetic fields and relative heating patterns due to a rectangular aperture source in direct contact with bilayered biological tissue," *IEEE Trans. Microwave Theory Tech*., vol. 29, pp. 214-223, 1971.

[46] D. V. Land, "Medical microwave radiometry and its clinical applications," *IEE Colloquium Application of Microwaves in Medicine*, pp. 2/1 - 2/5, 28 Feb 1995.

[47] B. Enander and G. Larson, "Microwave radiometry measurements of the temperature inside a body," *Electronic Letters*, vol. 10, pp. 317, 1974.

[48] J. Edrich and P. C. Hardee, "Thermography at millimeter wavelengths," *Proc. IEEE*, vol. 62, pp. 1391-1392, 1974.

[49] E. A. Cheever and K. R. Foster, "Microwave radiometry in living tissue: What does it measure?" *IEEE Trans. Biomedical Engineering*, vol. 39, no .6, pp. 563-568, June 1992.

[50] B. Bocquet, J. C. van de Velde, A. Mamouni, Y. Leroy, G. Giauz, J. Delannoy, and D. Delvalee, "Microwave Radiometric Imaging at 3 GHz for the Exploration of Breast Tumors," *IEEE Trans. Microwave Theory Tech.*, vol. 38, no.6, pp. 791-793, June 1990.

[51] L. Enel, Y. Leroy, J. C. Van de Velde, and A. Mamouni, "Improved recognition of thermal structures by microwave radiometry," *Electronics Letters*, vol. 20, pp. 293-294, 1984.

[52] Y. Leroy, A. Mamouni, J. C. Van de Velde, B. Bocquet, and B. Dujardin, "Microwave radiometry for non invasive thermometry," *Automedica (Special Issue on Noninvasive Thermometry)*, vol. 8, pp. 181-201, 1987.

[53] J. R. Hadley, B. E. Chapman, J. A. Roberts, D. C. Chapman, K. C. Goodrich, H. R. Buswell, A. L. Alexander, J. S. Tsuruda, and D. L. Parker, "A Three-Coil Comparison for MR Angiography," *Journal of Magnetic Resonance Imaging*, 11 pp. 458–468, 2000.

[54] C. E. Hayes, W. A. Edelstein, and J. F. Schenck, et al., "An efficient, highly homogeneous radiofrequency coil for whole-body NMR imaging at 1.5 T," *J. Magn. Reson. Imaging*, vol. 63, pp. 622–628, 1985.

[55] M. C. Leifer, "Theory of the quadrature elliptic birdcage coil," *Magn. Reson. Med.*, vol. 38 pp. 726–732, 1997.

[56] S. Li, C. M. Collins, and B. J. Dardzinski, et al., "A method to create an optimum current distribution and homogeneous B1 field for elliptical birdcage coils," *Magn. Reson. Med*., vol. 37, pp. 600–608,1997.

[57] J. R. Fitzsimmons, J. C. Scott, and D. M. Peterson, et al., "Integrated RF coil with stabilization for FMRI human cortex," *Magn. Reson. Med*., vol. 38, pp. 15–18, 1997.

[58] L. E. Hendrix, J. A. Strandt, and D. L. Daniels, et al., "Three-dimensional time-of-flight MR angiography with a surface coil: evaluation in 12 subjects," *American Journal Radiology*, vol. 159, pp. 103–106, 1992.

[59] P. B. Roemer, W. A. Edelstein, C. E. Hayes, S.P.Souza, and O.M.Mueller, "The NMR phased array, " *Magn. Reson. Med.*, 16(2), pp. 192-225, 1996.

[60] C. E. Hayes, N. Hattes, and P. B. Roemer, "Volume imaging with MR phased arrays," *Magn. Reson. Med*., vol. 18, no. 2, pp. 309-319,1991.

[61] C. E. Hayes and P. B. Roemer, "Noise correlations in data simultaneously acquired from multiple surface coil arrays," *Magn. Reson. Med.* , vol. 16, no. 2, pp. 181-191, 1991.

[62] S. M. Wright, R. L. Magin, and J. R. Kelton, "Arrays of mutually coupled receiver coils: theory and application," *Magn. Reson. Med.*, vol. 17, no. 1, pp. 252-268, 1991.

[63] S. M. Wright and L. L. Wald, "Theory and application of array coils in MR spectroscopy," *NMR Biomed.*, vol. 10, no. 8, pp. 394-410, 1997.

[64] G. R. Duensing, H. R. Brooker, and J. R. Fitzsimmons, "Maximizing signal-to-noise ratio in the presence of coil coupling," *Magn. Reson*. B, vol. 111, no. 3, pp. 230-235, 1996.

[65] D. K. Sodickson and W. J. Manning, "Simultaneous acquisition of spatial harmonics (SMASH): ultra-fast imaging with radiofrequency coil arrays," *Magn. Reson. Med.*, vol. 38, pp. 591-603, 1997.

[66] K. P. Pruessmann, M. Weiger, M. B. Scheidegger, and P. Boesiger, "SENSE: Sensitivity encoding for fast MRI," *Magn. Reson. Med.*, vol. 42, pp. 952-962, 1999.

[67] Y. Zhu, "Parallel excitation with an array of transmit coils," *Magn. Reson. Med.*, vol. 51, no. 4, pp. 775-784, 2004.

[68] K. Y. Kojima, J. Szumowski, and R. C. Sheley, et al., "Lower extremities: MRangiography with a unilateral telescopic phased-array coil," *Radiology*, 196, pp. 871–875, 1995.

[69] J. W. Monroe, P. Schmalbrock, and D. G. Spigos, "Phased array coils for upper extremity MRA," *Magn. Reson. Med.*, vol. 33, pp. 224–229, 1995.

[70] C. E. Hayes, C. M. Mathis, and C. Yuan, "Surface coil phased arrays for high-resolution imaging of the carotid arteries," *Magn. Reson. Imaging*, vol. 1, pp. 109–112, 1996.

[71] C. Yuan, J. W. Murakami, and C. E. Hayes, et al, "Phased-array magnetic resonance imaging of the carotid artery bifurcation: preliminary results in healthy volunteers and a patient with atherosclerotic disease," *Magn. Reson. Imaging*, vol. 5, pp. 561–565 1995.

[72] S. H. Faro, S. Vinitski, and H. V. Ortega, et al, "Carotid magnetic resonance angiography: improved image quality with dual 3-inch surface coils," *Neuroradiology*, vol. 38, pp. 403–408, 1996.

[73] H. A. Stark and E. M. Haacke, "Helmet and cylindrical shaped CP array coils for brain imaging: a comparison of signal-to-noise characteristics," *Proceedings of the International Society for Magnetic Resonance in Medicine*, pp. 1412, 1996.

[74] J. R. Porter, S. M. Wright, and A. Reykowski, "A 16-element phased-array head coil," *Magn. Reson. Med.*, vol. 40, pp. 272–279, 1998.

[75] T. Wu and R. King, "The cylindrical antenna with nonreflecting resistive loading," *IEEE Trans. Antennas Propag.*, vol. AP-13, no. 3, pp. 369–373, May 1965.

[76] T. Wu and R. King, "Corrections to 'The cylindrical antenna with nonreflecting resistive loading'," *IEEE Trans. Antennas Propag*., vol. AP-13, no. 11, p.998, Nov. 1965.

[77] E. C. Fear, J. Sill, and M. A. Stuchly, "Experimental Feasibility Study of Confocal Microwave Imaging for Breast Tumor Detection ," *IEEE Trans. Microwave Theory Tech*., vol. 51, no. 3, pp. 887-892, March 2003.

[78] *Special Issue of IEEE Trans. Microwave Theory Tech*., MTT-34, 1986.

[79] C. H. Durney and M. F. Iskander, *Antenna Handbook*. Eds. Y.T. Lo & S.W. Lee, 1993.

[80] P. K. Sneed and T. L. Phillips, "Combining hyperthermia and radiation: How beneficial?," *Oncology*, vol. 5, pp. 99-108, 1991.

[81] C. C. Vernon, J. W. Hand, and S. B. Field, et al., "Radiotherapy with or without hyperthermia in the treatment of superficial localized breast cancer: Results from five randomized controlled trials," *Int. J. Radiat. Oncol. Biol. Phys*., vol. 35, pp. 731-44, 1996.

[82] F. Monteccia, "Microstrip antenna design for hyperthermia treatment of superficial tumors," *IEEE Trans. BME*, vol. 39, no. 6, pp. 580-588, June 1992,

[83] J. Vba, C. Franconi, F. Montecchia, and I. Vannucci, "Evanescent-Mode Applicators (EMA) for superficial and subcutaneous hyperthermia," *IEEE Trans. Biomed. Eng*., vol. 40, no.5, pp. 397-407, May 1993.

[84] M. V. Prior, M. L. D. Lumori, J. W. H, G. Lamaitre, C. J. Schneider, and J. D. P. van Dijk, "The Use of a Current Sheet Applicator Array for Superficial Hyperthermia: Incoherent Versus Coherent Operation," *IEEE Trans. Biomed. Eng*., vol. 43, no. 7, pp. 694-698, July 1995.

[85] P. R. Stauffer, M. Leoncini, and V. Manfrini, et al., "Dual concentric conductor radiator for microwave hyperthermia with improved field uniformity to periphery of aperture," *IEICE Trans. on Communicat.*, vol. E78-B, pp. 826-35, 1995.

[86] P. F. Maccarini, H. Rolfsnes, D. Neuman and P. Stauffer, "Optimization of a Dual Concentric Conductor Antenna for Superficial Hyperthermia Applications," *Proceedings of the 26th Annual International conference of the IEEE EMBS*, San Francisco, CA, USA , September 1-5, 2004.

[87] S. Jacobsen, P. R. Stauffer, and D. G. Neuman, "Dual-mode antenna design for microwave heating and noninvasive thermometry of superficial tissue disease," *IEEE Trans. Biomed. Eng*., vol. 47, 2000.

[88] P. F. Turner, "Interstitial Equal-Phased Arrays for EM Hyperthermia," *IEEE Trans. Microwave Theory and Tech*., vol. 34, no.5, pp. 572 - 578, May 1986.

[89] C. M. Furse and M. F. Iskander, "Three-dimensional Electromagnetic Power Deposition in Tumors using Interstitial Antenna Arrays,"

IEEE Trans. on Biomedical Engineering, vol. 36, pp. 977-986, Oct. 1989.

[90] P. Cherry and M. F. Iskander, "FDTD analysis of power deposition patterns of an array of interstitial antennas for use in microwave hyperthermia," *IEEE Trans. Microwave Theory and Tech,* vol. 40, no. 8, pp. 1692-1700, Aug 1992.

[91] R. D. Nevels, G. D. Arndt, G. W. Raffoul, J. R. Carl, and A. Pacifico, "Microwave catheter design," *IEEE Trans. on Biomedical Engineering*, vol. 45, pp.885–890, July 1998.

[92] C. Manry, S. L. Broschat, C.-K. Chou, and J. A. McDougall, "An eccentrically coated asymmetric antenna applicator for intracavity hyperthermia treatment of cancer," *IEEE Trans. on Biomedical Engineering*, vol. 39, no. 9, pp. 935-942, Sept. 1992.

[93] J. C. Camart, D. Despretz, M. Chive, and J. Pribetich, "Modeling of various kinds of applicators used for microwave hyperthermia based on the FDTD method," *IEEE Trans. Microwave Theory and Tech*., vol. 44, no. 10, pp. 1811-1818, Oct. 1996.

[94] P. F. Turner, "Hyperthermia and Inhomogeneous Tissue Effects Using an Annular Phased Array," *IEEE Trans. Microwave Theory and Tech*., vol. 32, no. 8, pp. 874 - 875, Aug. 1984.

[95] P. Stauffer, J. Schlorff, R. Taschereau, T. Juang, D. Neuman, P. Maccarini, J. Pouliot and J. Hsu, "Combination Applicator for Simultaneous Heat and Radiation," *Proceedings of the 26th Annual International Conference of the IEEE EMBS*, San Francisco, CA, September 1-5, 2004.

[96] Y. Kotsuka, E. Hankui, and Y. Shigematsu, "Development of Ferrite Core Applicator System for Deep-Induction Hyperthermia," *IEEE Trans. Microwave Theory and Tech*., vol. 44, no. 10, pp. 1803-1810, Oct. 1996.

[97] D. M. Sullivan, "Three-dimensional computer simulation in deep regional hyperthermia using the FDTD Method," *IEEE Trans. Microwave Theory and Tech*., vol. 38, no. 2, pp. 201-211, Feb. 1990.

[98] P. F. Turner, "Sigma 60–24 Prototype Test Results," *BSD Medical Corporation*, Salt Lake City, UT, Internal Rep., 1992.

[99] J. Nadobny, H. Fähling, M. Hagmann, P. Turner, W. Wlodarczyk, J.Gellermann, P. Deuflhard, and P. Wust, "Experimental and numerical investigations of feed-point parameters in a 3-D hyperthermia applicator using different models of feed networks*," IEEE Trans. Biomed. Eng*., vol. 49, no. 11, pp. 1348–1359, Nov. 2002.

[100] J. Nadobny, W. Wlodarczyk, L. Westhoff, J. Gellermann, R. Felix, and P. Wust, "A Clinical Water-Coated Antenna Applicator for MR-Controlled Deep-Body Hyperthermia: A Comparison of Calculated and Measured 3-D Temperature Data Sets," *IEEE Trans. on Biomedical Engineering*, vol. 52, no. 3, pp. 505-519, March 2005.

[101] K. S. Nikita and N. K. Uzunoglu, "Coupling Phenomena in Concentric Multi-Applicator Phased Array Hyperthermia Systems," *IEEE Trans. Microwave Theory and Tech*., vol. 44, no. 1, pp. 65-74, Jan 1996.

[102] F. Bardati, A. Borrani, A. Gerardino, and G. A. Lovisolo, "SAR Optimization in a Phased Array Radiofrequency Hyperthermia System," *IEEE Trans. on Biomedical Engineering*, vol. 42, no. 12, pp. 1201-1207, Dec. 1995.

[103] R. W. P. King, G. J. Fikioris, and R. B. Mack, *Cylindrical Antennas and Arrays*, Cambirdge, U.K.: Cambridge Univ. Press, 2002.

[104] S. Ebihara and T. Yamamoto, "Resonance analysis of a circular dipole array antenna in cylindrically layered media for directional borehole radar," *IEEE Trans. Geosci. Remote Sensing*, vol. 44, no.1, pp. 22-31, Jan. 2006.

[105] K. Holliger and T. Bergmann, "Numerical modeling of borehole geo-radar data," *Geophysics*, vol. 67, no. 4, pp. 1249-1257, July/Aug. 2002.

[106] J. R. Hadley, "Design of Radio Frequency Coil Arrays for Optimal Signal to Noise Ratio for Magnetic Resonance Angiography," PhD Dissertation, University of Utah Electrical and Computer Engineering Department, 2005.

[107] H. Massoudi, C. H. Durney, and M. F. Iskander, "Limitations of the cubical block model of man in calculating SAR distribution," *IEEE Trans. Microwave Theory and Tech.*, vol. 32, pp. 746-752, 1984.

[108] C. T. Tsai, H. Massoudi, C. H. Durney, and M. F. Iskander, "A procedure for calculating fields inside arbitrarily-shaped, inhomogeneous dielectric bodies using linear basis functions with the moment method," *IEEE Trans. Microwave Theory and Tech*., vol. 34, pp. 1131-1139, 1986.

[109] O. H. Schaubert, D. R. Wilton, and A. W. Glisson, "A tetrahedral modeling method of electromagnetic scattering by arbitrarily shaped inhomogeneous objects," *IEEE. Trans. Antennas and Propagation*, vol. 32, pp. 75-82, 1984.

[110] B. M. Green and M. A. Jensen, "Diversity performance of dual-antenna handsets near operator tissue," *IEEE. Trans. Antennas and Propagation*, vol. 48, no. 7, pp. 1017-1024, July 2000.

[111] O. Gandhi, G. Lazzi, and C. Furse, "Electromagnetic Absorption in the Human Head

and Neck for Mobile Telephones at 835 and 1900 MHz," *IEEE Trans. on Microwave Theory and Tech*., vol. 44, pp. 1884 -1897, 1996.

[112] P. Soontornpipit, C. M. Furse, and Y. C. Chung , "Design of Implantable Microstrip Antenna for Communication with Medical Implants*," Special Issue of IEEE Trans. on Microwave Theory and Tech. on Medical Applications and Biological Effects of RF/Microwaves* , Sept. 2004.

[113] C. E. Reuter, A. Taflove, V. Sathiaseelan, M. Piket-May, and B. B. Mittral, "Unexpected physical phenomena indicated by FDTD modeling of the Sigma-60 deep hyperthermia applicator," *IEEE Trans. Microwave Theory and Tech*., vol. 46, no.4, pp. 313-319, April 1998.

[114] C.-Q. Wang and O. P. Gandhi, "Numerical simulation of annular phased arrays for anatomically based models using the FDTD method," *IEEE Trans. Microwave Theory and Tech*., vol. 37, no.1, pp. 118-126, Jan, 1989.

[115] D. Sullivan, D. Buechler, and F. A. Gibbs, "Comparison of measured and simulated data in an annular phased array using an inhomogeneous phantom," *IEEE Trans. Microwave Theory and Tech*., vol. 40, no.3, pp. 600-604, Mar. 1992.

[116] C. M. Furse, J.-Y. Chen, and O. P. Gandhi, "Use of the Frequency-Dependent Finite-Difference Time-Domain Method for Induced Current and SAR Calculations for a Heterogeneous Model of the Human Body," *IEEE Trans. on Electromagnetic Compatibility*, pp.128-133, May 1994.

[117] C. Furse and O. P. Gandhi, "Calculation of Electric Fields and Currents Induced in a Millimeter-Resolution Human Model at 60 Hz Using the FDTD Method," *Bioelectromagnetics*, 19 (5), pp.293-299, 1998.

[118] C. M. Furse and O. P. Gandhi, "A Memory Efficient Method of Computing Specific Absorption Rate in CW FDTD Simulations," *IEEE Transactions on Biomedical Engineering*, vol. 43, no. 5, pp. 558-560, May 1996.

[119] C. H. Durney, C. C. Johnson, P. W. Barber, H. Massoudi, M. F. Iskander, J. L. Lords, D. K. Ryser, S. J. Allen, and J. C. Mitchell, *Radiofrequency Radiation Dosimetry Handbook*, 2nd ed., USAF School of Medicine, Brooks AFB, TX, 1978.

[120] O. P. Gandhi, , Y. G. Gu, J. Y. Chen, and H. I. Bassen, "Specific absorption rates and induced current distributions in an anatomically based human model for plane-wave exposures," *Health Physics*, 63(3), pp. 281-290, 1992.

[121] O. P. Gandhi and C. M. Furse, "Millimeter-resolution MRI-based models of the human body for electromagnetic dosimetry from ELF to microwave frequencies," *Voxel Phantom Development: Proceedings of an International Workshop held at the National Radiological Protection Board*, Chilton, UK, July 6-7, 1995, Peter J. Dimbylow, editor.

[122] P. J. Dimbylow, "The development of realistic voxel phantoms for electromagnetic field dosimetry," *Voxel Phantom Development: Proceedings of an International Workshop held at the National Radiological Protection Board*, Chilton, UK, July 6-7, 1995, Peter J. Dimbylow, editor.

[123] P. Olley and P. S. Excell, "Classification of high resolution voxel image of a human head," *Voxel Phantom Development: Proceedings of an International Workshop held at the National Radiological Protection Board*, Chilton, UK, July 6-7, 1995, Peter J. Dimbylow, editor.

[124] M. A. Stuchly, K. Caputa, A. van Wensen, and A. El-Sayed, "Models of human and animal bodies in electromagnetics," *Voxel Phantom Development: Proceedings of an International Workshop held at the National Radiological Protection Board*, Chilton, UK, July 6-7, 1995, Peter J. Dimbylow, editor.

[125] National Library of Medicine, Visible Man Project, MRI scans, CT scans, and photographs available on CD through Research Systems, Inc., 2995 Wilderness Place, Boulder, CO 80301.

[126] C. Gabriel, "Compilation of the dielectric properties of body tissues at RF and microwave frequencies," *Final Report AL/OE-TR-1996-0037 submitted to Occupational and Environmental Health Directorate, RFR Division*, 2503 Gillingham Dr., Brooks AFB, TX, June 1996.

[127] M. A. Stuchly and S. S. Stuchly, "Dielectric properties of biological substances – tabulated," *J. Microwave Power*, 15 (1), pp. 19-26, 1980.

[128] S. Rush, J. A. Abildskov, and R. McFee, "Resistivity of body tissues at low frequencies," *Circ. Research*, vol. XII, pp. 40-50, 1963.

[129] L. A. Geddes and L. E. Baker, "The specific resistance of biological material – a compendium of data for the biomedical engineer and physiologist," *Med. & Biol. Engng*., vol. 5, pp. 271-293, Pergamon Press., 1967.

[130] University of Utah Dielectric Database OnLine http://www.ece.utah.edu/dielectric/

[131] D. M. Pozar, "Microstrip antennas," *Proc. IEEE*, vol. 80, pp. 79-91, Jan 1992.

[132] A. Cucini, M. Albani, and S. Maci, "Truncated floquet wave full-wave analysis of large phased arrays of open-eneded waveguides with nonuniform amplitude excitation," *IEEE Trans. Antennas and Propagation*, vol. 51, no.6, pp. 1386-1394, June 2003.

[133] G. Turner and C. Christodoulou, "FDTD analysis of phased array antennas," *IEEE Trans. Antennas and Propagation*, vol. 47, no. 4, pp. 661-667, April 1999.

[134] J. Ren, O. P. Gandhi, L. R. Walker, J. Fraschilla, and C. R. Boerman, "Floquet-based FDTD analysis of two-dimensional phased array antennas," *IEEE Microwave and Guided Wave Letters*, vol. 4, no.4, pp. 109-111, April 1994.

[135] C. Railton and G. S. Hilton, "The analysis of medium-sized arrays of complex elements using a combination of FDTD and reaction matching," *IEEE Trans. Antennas and Propagation*, vol. 47, no. 4, pp. 707-714, April 1999.

[136] J. Gomez-Tagle, P. Wahid, M. Chriyssomallis, and C. Christodoulou, "FDTD analysis of finite-sized phased array microstrip antennas," *IEEE Trans. Antennas and Propagation*, vol. 51, no. 8, pp. 2057-2062, Aug. 2003.

[137] H. Holter and H. Steyskal, "On the size requirement for finite phased-array models," *IEEE Trans. Antennas and Propagation*, vol. 50, no. 6, pp. 836-840, June 2002.

[138] T. Su, N.-T. Huang, Y. Lio, W. Yu, and R. Mittra, "Investigation of instability characteristics arising in the FDTD simulation of electrically large antenna arrays," *IEEE Antennas and Propagation Society International Symposium*, vol. 1, pp. 1014-1017, June 2004.

Dr. Cynthia Furse is the Director of the Center of Excellence for Smart Sensors at the University of Utah and Professor in the Electrical and Computer Engineering Department. The Center focuses on imbedded antennas and sensors in complex environments, such as telemetry systems in the human body, and sensors for location of faults on aging aircraft wiring. Dr. Furse has directed the Utah "Smart Wiring" program, sponsored by NAVAIR and USAF, since 1998. She is Head of Research for LiveWire Test Labs, Inc., a spin off company commercializing devices to locate intermittent faults on live wires. Dr. Furse teaches electromagnetics, wireless communication, computational electromagnetics, microwave engineering, and antenna design. Dr. Furse was the Professor of the Year in the College of Engineering at Utah State University for the year 2000, and Faculty Employee of the year 2002. She is the chair of the IEEE Antennas and Propagation Society Education Committee, and associate editor of the IEEE Transactions on Antennas and Propagation.